Applied Catalysis B: Environmental 172–173 (2015) 108–115

Contents lists available at ScienceDirect

Applied Catalysis B: Environmental

journal homepage: www.elsevier.com/locate/apcatb

Esterification of palmitic acid with methanol over template-assisted mesoporous sulfated zirconia solid acid catalyst

K. Saravanan[a,b], Beena Tyagi[a,b,*], Ram S. Shukla[a,b], H.C. Bajaj[a,b]

[a] Discipline of Inorganic Materials and Catalysis, CSIR-Central Salt and Marine Chemicals Research Institute (CSIR-CSMCRI), G.B. Marg, Bhavnagar 364 002, India

[b] Academy of Scientific and Innovative Research (AcSIR), CSIR-Central Salt and Marine Chemicals Research Institute (CSIR-CSMCRI), G.B. Marg, Bhavnagar 364 002, Gujarat, India

ARTICLE INFO

Article history:
Received 18 November 2014
Received in revised form 26 January 2015
Accepted 11 February 2015
Available online 14 February 2015

Keywords:
Sulfated zirconia
Palmitic acid
Esterification
Methyl palmitate
CTAB template

ABSTRACT

The esterification of palmitic acid with methanol was studied over mesoporous sulfated zirconia (SZ) solid acid catalyst, prepared by using CTAB cationic surfactant as a template. The effect of various reaction parameters has been studied. The catalyst showed an excellent activity with 88–90% yield of methyl palmitate at 60 °C after 5–7 h. The reaction follows pseudo-first order kinetics under the reaction conditions studied with a reaction rate of 48.67 mmol h^{-1} g^{-1} and turnover frequency of 6.96 h^{-1}. It is noteworthy that SZ catalyst showed comparable activity to conventional Brönsted acids namely H_2SO_4 and *p*-TSA; as well as it exhibited higher activity than various other heterogeneous catalysts such as zeolites, ion-exchange resins and acid clay.

1. Introduction

Fatty acid alkyl esters, which are commonly known as biodiesel, are synthesized either from the esterification of free fatty acids using acid catalysts or the transesterification of renewable biological sources namely triglycerides with base catalysts. Generally, low-cost feedstocks like non-edible oils and waste cooking oils are having more free fatty acid contents which lead to soap formation with base catalyst during transesterification reaction [1]. Thus, industrial production of biodiesel from such oils having higher free fatty acids requires two-step process, wherein, esterification of free fatty acids with acid catalyst is done in the first step followed by subsequent transesterification with base catalyst in the second step [2]. Therefore, acid catalyzed esterification of long-alkyl chain fatty acids has prompted a great deal of interest over the base catalyzed transesterification reaction [3]. Palmitic acid or hexadecanoic acid ($C_{16}H_{32}O_2$) is a saturated fatty acid naturally occuring in all edible and non-edible oils in varying amounts (4–23%) [3]. Among various saturated fatty acids (C_8–C_{18}) present in oils and grease, the amount of palmitic acid is generally higher [3]. It is a major component (48%) of palm oil among total saturated fatty acids (54%) [4]. Palmitic acid is also the most common saturated fatty acid found in animals, plants and microorganisms and also in milk, cheeses, butter and meats [5].

Conventionally, industrial esterification processes are carried out in the presence of homogeneous Brönsted acid catalysts such as sulfuric, *p*-toluene sulfonic or phosphoric acid. These liquid inorganic acid catalysts lead to corrosion problems and need to be neutralized at the end of the reaction resulting in large salt generation and loss of required yield. The waste generated in multi-product industries ranges from 10 to 100 kg per kg of the anticipated product depending on the number of steps of the process [6]. Thus the extensive demand for cleaner methodologies emerged eco-friendly heterogeneous acid catalysts that can be easily separable and re-usable [7,8].

A number of solid acid catalysts have been studied for the esterification of fatty acids such as zeolite, ion-exchange resins, sulfated metal oxides [9], sulfonated carbon sugar [10], organosulfonic acid mesoporous silica [1,11], Fe–Zn double-metal cyanide [12], and Brönsted acid ionic liquids [13] *etc*. The reported studies reveal that various solid acid catalysts showed good catalytic activity for the esterification of palmitic acid; however, the studies have been carried out at varied range of reaction variables. For example, acid to methanol ratio was used in the range of 1:1.2–1:40, reaction temperature from 50 to 200 °C over 2–15 wt%

* Corresponding author at: Discipline of Inorganic Materials and Catalysis, Council of Scientific and Industrial Research (CSIR), Central Salt and Marine Chemicals Research Institute (CSIR-CSMCRI), G.B. Marg, Bhavnagar, Gujarat 364 002, India. Tel.: +91 278 2567760; fax: +91 278 2566970.
E-mail address: btyagi@csmcri.org (B. Tyagi).

http://dx.doi.org/10.1016/j.apcatb.2015.02.014
0926-3373/

catalyst amount. An exceptionally high amount of catalyst such as 75 wt% (tungstated zirconia) [14], and 100 wt% (sulfonated single-walled carbon nanohorn catalyst) [15] along with a very high acid to methanol ratio of 1:200 and 1:270, have also been reported to achieve 90–95% conversion of palmitic acid. Many other catalysts have been found to exhibit significant conversion (80–100%) of palmitic acid but a higher acid to methanol ratio was required, for example, 1:40 (MCM-41 supported 12-tungstophosphoric acid, TPA) [16], 1:60–1:66 (Al-MCM-41 [17], $WO_x/ZrPO_4$ [18] and glycerol-based carbon catalyst [19]), 1:79 (silica supported heteropolyacid, HPA) [20], 1:98 (sulfonated chitosan [21a] and polyvinyl alcohol cross-linked with sulfosuccinic acid [21b], silica supported HPA) [22], 1:120 (tin phosphonate monolith) [23], 1:98–1:200 (silica [24]/niobia [25a] supported 12-TPA and ammonium salt of 12-TPA [25b]). In addition, higher reaction temperature of 130–200 °C [17,20,26] and longer reaction time of 24–30 h [18,21b,27] were required to obtain maximum conversion with these catalysts. However, such a high acid to methanol ratio, time and temperature is not feasible from economic and industrial point of view.

Recently, we obtained excellent activity of sulfated zirconia (SZ) catalyst for esterification of myristic acid with methanol [28]. In the present study, we report a systematic detailed study of the esterification of palmitic acid with methanol at lower temperature and acid to methanol ratio over mesoporous SZ catalyst, prepared by template-assisted method. The effects of various reaction variables such as acid to methanol molar ratio, catalyst amount, reaction temperature, time and stirring speed along with other short chain alcohols namely ethanol, *n*-propanol and *n*-butanol have been investigated. The efficiency of SZ catalyst after its re-use along with the comparison of its catalytic activity with other heterogeneous catalysts has also been addressed. To the best of our knowledge, no systematic detailed study has been stated on the esterification of palmitic acid with methanol using SZ catalyst so far.

2. Experimental

2.1. Catalyst synthesis

SZ catalyst was prepared by template-assisted method using cetyltrimethyl ammonium bromide (CTAB) cationic surfactant as a template [29]. In a typical procedure, CTAB (5 g, 98%, Spectrochem Pvt., Ltd.) was dissolved in a solution of water (230 g) and HCl (49 g, 37%, Fisher Scientific) under stirring. $Zr(OPr)_4$ (70 wt%, 12 g, Sigma–Aldrich), diluted to 30 wt% by *n*-propanol (28 g, 99%, Fisher Scientific), was added into CTAB solution. To this $(NH_4)_2SO_4$ (4 g, 99.5%, Rankem) in water (46 g) was added and the mixture was stirred at room temperature (~27 °C) for 1 h. The clear solution was then heated in an autoclave at 100 °C for 2 days. The white precipitate obtained was washed with water, filtered, dried and calcined at 600 °C for 5 h under air flow.

2.2. Catalyst characterization

The crystalline phase of the prepared SZ catalyst was analyzed by Philips X'pert powder diffractometer (The Netherlands). The crystallite size was determined from the characteristic peak of tetragonal phase ($2\theta = 30.2^\circ$) using Scherrer equation [30]: crystallite size $= K\lambda/W \cos\theta$, where K is the Scherrer constant (0.9), $\lambda = 1.5406$ Å (CuKα radiation), $W = Wb - Ws$; Wb is the broadened profile width of experimental sample and Ws is the standard profile width of reference silicon sample and θ is the angle of diffraction. FT-IR spectrum was recorded on a PerkinElmer GX spectrophotometer (USA) in the range of 400–4000 cm^{-1} with a resolution of 4 cm^{-1} as KBr pellets. The bulk sulfur present in sample before calcination and retained after calcination was analyzed by PerkinElmer 2400 elemental analyzer (USA). The sulfate and Zr contents were analysed by ion chromatography (Dionex ICS 3000) and inductively coupled plasma (ICP) atomic emission spectrometer (PerkinElmer, Optima 2000 DV), respectively.

BET surface area, pore volume and pore diameter were calculated from N_2 sorption isotherms at −196 °C using ASAP 2010, Micromeritics (USA) after pre-activation under vacuum (1×10^{-3} mmHg) at 150 °C for 4 h. Surface area and pore size were calculated by BET (Brunauer–Emmett–Teller) equation and BJH (Barrett–Joyner–Halenda) method, respectively [31].

SEM and TEM micrographs were obtained using a Leo series VP1430 scanning electron microscope (Germany) and a Jeol JEM 2100 transmission electron microscope (USA), respectively. The catalyst sample was dispersed in ethanol by sonication and deposited on an Al grid coated with gold using a Polaron Sputter Coater (for SEM) and on a Cu grid coated with carbon film (for TEM).

The total surface acidity, *i.e.*, strength and number of acid sites present in the catalyst was measured by NH_3-TPD using Micromeritics AutoChem II (USA). In a typical procedure, a mixture of 10% NH_3 and He gas was passed for 30 min at 40 °C over the sample (*in situ* activated at 120 °C for 2 h). The excess physisorbed NH_3 was flushed out for 10 min with pure He gas flow. The sample was then heated at a rate of 10 °C min^{-1} up to 800 °C and volume of desorbed NH_3 was measured.

Vapor phase cyclohexanol dehydration to cyclohexene in a fixed bed reactor was used as a model reaction to assess the Brönsted acidity of the catalyst [32]. Cyclohexanol (2 ml) was delivered by a syringe pump injector (Cole Parmer, 74,900 series) with a flow rate of 1 ml h^{-1} under N_2 at 175 °C over the catalyst sample (0.2 g) (*in situ* activated at 450 °C for 2 h) packed in a reactor bed. Product samples were collected after 1 h and analyzed with a Hewlett-Packard gas chromatogram (HP 6890) having FID detector. The conversion of cyclohexanol and selectivity for cyclohexene was calculated by GC on weight percent basis.

Brönsted (B) and Lewis (L) acid sites were differentiated by pyridine adsorbed SZ samples using PerkinElmer GX spectrophotometer equipped with Diffuse Reflectance FT-IR (DRIFT) accessory (Graseby Specac, P/N 19,900) and a temperature controller (Graseby Specac, P/N 20,130) [33]. The sample was exposed to *ex-situ* pyridine vapor under vacuum for 1 h followed by evacuation of excess physisorbed pyridine for 10 min. The spectra were recorded at room temperature (~27 °C) and in the temperature range of 150–450 °C after holding at each temperature for 10 min, thus allowing sufficient time for pyridine desorption at that temperature.

The quantification of B and L acid sites ratio (B/L) was done from the characteristic peak area of 1545 cm^{-1} for B and 1442 cm^{-1} for L at 150 °C [33] as well as by molar extinction coefficient ($\epsilon_B = 1.67$ cm/μmol and $\epsilon_L = 2.22$ cm/μmol) method using the following equations [34,35]:

$$C = \frac{IA\pi R^2}{W\epsilon} \quad (1)$$

By using $\epsilon_B = 1.67$ cm/μmol and $\epsilon_L = 2.22$ cm/μmol in Eq. (1), following equations are derived [34]:

$$C_B = \frac{1.88 IA_B R^2}{W} \quad (2)$$

$$C_L = \frac{1.42 IA_L R^2}{W} \quad (3)$$

where $C_{B,L}$ = concentration of B and L acid sites (mmol/g); IA = integrated absorbance ($IA_B = 20.7$ cm^{-1}; $IA_L = 20$ cm^{-1}); R = radius of catalyst disk (0.43 cm) and W = weight of catalyst (0.164 g).

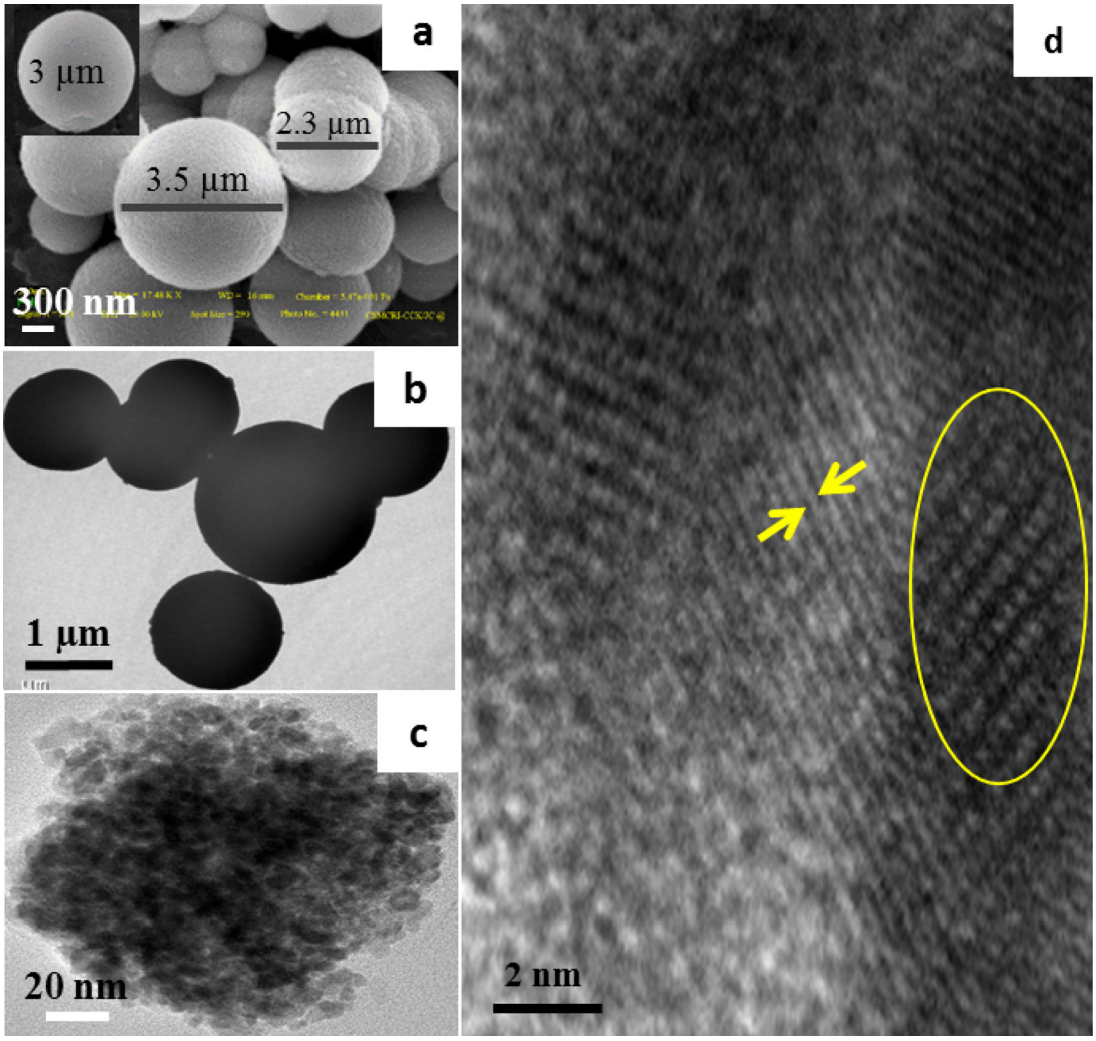

Fig. 1. (a) SEM, (b) TEM, and (c,d) HR-TEM images of SZ catalyst; (d) ordered porous structure (circled) and lattice fringes of lamellar structure (marked by arrow).

2.3. Catalytic activity

The catalytic activity of prepared SZ catalyst was evaluated for the esterification of palmitic acid (PA) with methanol along with other short chain alcohols in a liquid phase batch reactor. In a typical reaction procedure, 3 mmol of PA (0.775 g, 99%, SRL Pvt., Ltd.), 60 mmol of methanol (1.98 g, 99.8%, SRL Pvt., Ltd.) and desired amount of SZ catalyst were taken in a round bottom flask and the reactant mixture was magnetically stirred (700 rpm) in an oil bath maintained at constant temperature of 60 ± 1 °C for 7 h. The catalyst was separated from the reaction mixture by centrifugation and methyl palmitate (MP) was obtained after removal of methanol by rotatory evaporator. The yield of MP (%) was analyzed by ^{1}H NMR in chloroform-*d* (99.8%, Aldrich) solvent using following equation:

$$\text{Yield of methyl palmitate (\%)} = 100 \times \left(\frac{2A_{ME}}{3A_{\alpha-CH_2}} \right)$$

where A_{ME} = integrated area of methoxy hydrogen (CH_3O—) signal at 3.66 ppm and $A_{\alpha-CH_2}$ = integrated area of α-methylene hydrogen (at α-position to the carbonyl group) at 2.26–2.38 ppm. The factors 2 and 3 are derived from the fact that the methylene carbon possesses two hydrogen atoms and the methyl (methanol derived) carbon has three attached hydrogen atoms [36]. The yield of other alkyl (*C* = 2,3,4) palmitate (%) was estimated by the equation given below:

$$\text{Yield of alkyl palmitate (\%)} = 100 \times \left(\frac{A_{CH_2-OR}}{A_{\alpha-CH_2}} \right)$$

where A_{CH_2-OR} is the area of methylene protons (4.2–4.0 ppm) of the ethoxy, propoxy and butoxy group in the ester ($R = C_2H_4, C_3H_7, C_4H_9$) and $A_{\alpha-CH_2}$ is the total area of α-CH_2 signals (2.4–2.2 ppm) of acid and ester [36].

The acid base titration with 0.1 N alcoholic KOH using phenolphthalein indicator has also been done with time to estimate the conversion of palmitic acid on the basis of acid value. For kinetic studies, aliquots were taken at desired time and concentration of PA and MP were determined to find out the rates, ν and ν_1, and rate constants, k [36].

3. Results and discussion

3.1. Catalyst characterization

A SEM micrograph of the prepared SZ catalyst showed spherical morphology (Fig. 1a) as aggregates as well as isolated spherical particle (inset of Fig. 1a). The particles were found to have the size in the range of 1.2–3.5 μm with an average size of ~2.3 μm. A TEM micrograph (Fig. 1b) also showed the spherical SZ particles.

The high-resolution TEM (HR-TEM) images displayed the aggregate of crystallites within a particle (Fig. 1c) and the structure of the pores (Fig. 1d). Fig. 1d clearly exhibited ordered porous structure along with lamellar structure. Similar structure has been observed by CTAB-assisted porous zirconia-based material [29]. The width between two lattice fringes (2.95 Å) of lamellar structure agreed with *d*-spacing (2.96 Å) of characteristic peak of tetragonal zirconia ($^{\circ}2\theta$ = 30.2) shown by PXRD. The average crystallite size calculated by HR-TEM was 8.2 nm. The use of CTAB surfactant during the synthesis forms the micelle that prevents the agglomerization of zirconia particles and thus leads to the formation of particles of smaller size.

A powder X-ray diffraction (PXRD) pattern of SZ catalyst showed predominantly tetragonal crystalline phase ($^{\circ}2\theta$ = 30.2, 35.3, 50.3, 60.2, 62.8) after calcination at 600 °C (Fig. S1). The crystallite size calculated by Scherrer equation was of 9.2 nm, which was in close agreement with HR-TEM analysis.

The FT-IR-spectrum (Fig. S2) exhibited the bands at 1240, 1140, 1071, 1044 and 996 cm^{-1}, characteristic of inorganic chelating bidentate sulfate having asymmetric and symmetric stretching frequencies of S⋯O and S—O bonds with C_{2v} symmetry and ν_3 and ν_1 stretching mode of SO_4^{2-} groups [37]. The absence of covalent S═O band at ~1400 cm^{-1} suggested the partial ionic nature and hydrated state of sulfate groups at the surface of zirconia. A broad peak at ~3400 cm^{-1} attributed to ν_{O-H} stretching mode of water with hydrogen bonding and a peak at ~1630 cm^{-1} for δ_{O-H} bending mode of water molecules associated with the sulfate group and zirconia surface was also observed (not shown).

The total bulk sulfur content loaded in the sample before calcination was 1.44 mmol/g, which was decreased to 0.45 mmol/g, after calcination at 600 °C due to removal of sulfur content by heating the sample at higher temperature (Table 1). The Zr and sulfate contents of calcined sample were found to be 7.87 and 3.83 mmol/g respectively thus showing Zr:SO_4 ratio of 2.

N_2 sorption isotherm of the catalyst showed a well-defined type IV isotherm of mesoporous materials (Fig. S3a) with complete absence of micropores [31]. A sharp hysteresis of type H2 at 0.4 to 0.6 relative pressures indicated the presence of larger pores with uniform pore size distribution (Fig. S3b). *t*-plot analysis also confirmed the absence of micropores. In general, calcination of metal oxide material at higher temperature results into a partial collapsing of pores leading to the formation of micropores. However, formation of CTAB micelles during the synthesis of SZ material prevents the agglomerization of zirconia particle resulting into the formation of larger pores after its removal. The catalyst has good BET surface area (111 m^2/g) and mesopore volume (0.095 cm^3/g) having average pore diameter of 4.7 nm (Table 1).

The total surface acidity of SZ catalyst analyzed by NH_3-TPD was 1.65 mmol/g (Table 1). NH_3-desorption peaks showed the presence

Table 1
Physico-chemical characterization of SZ catalyst.

Crystallite size (nm)	8.2[a] (9.2[b])
Sulfur (mmol/g)	0.45
BET surface area (m^2/g)	111
Average pore volume (cm^3/g)	0.095
t-plot micropore volume (cm^3/g)	nil
BJH pore diameter (nm)	4.7
Cyclohexanol conversion (%)	94
Total acid sites (mmol/g)	1.65
Acid site density (mmol/m^2)	0.015
Bronsted acid sites (mmol/g)	0.044[c]
Lewis acid sites (mmol/g)	0.032[c]
B/L ratio	1.38[c] (1.42[d])

[a] By TEM.
[b] By Scherrer formula in PXRD.
[c] By molar extinction coefficient method.
[d] By characteristic peak area.

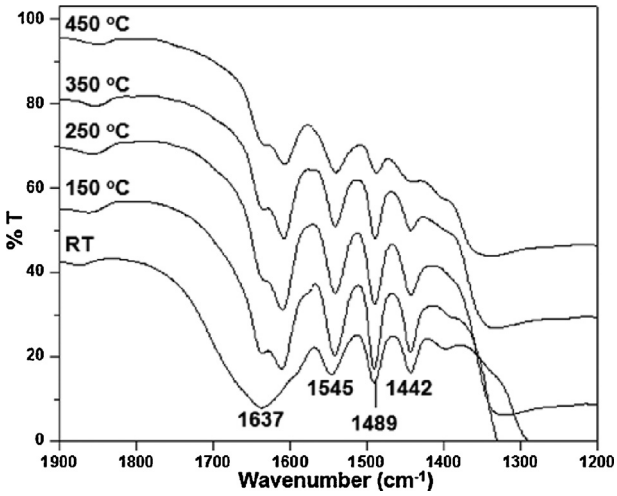

Fig. 2. DRIFT spectra of SZ catalyst after pyridine adsorption at room temperature (RT) and desorption at 150–450 °C.

of weak (98 °C), moderate (525 °C) and strong (794 °C) acid sites (Fig. S4). The number of acid sites present was in the following order: weak > strong > moderate. The less acid site density per unit surface area (0.015 mmol/m^2) indicated that acid sites are not dense and so there may be no/lower steric hindrance of reactant molecules to approaching the acid sites.

The dehydration of cyclohexanol showed 94% conversion of cyclohexanol (Table 1) with 100% selectivity for cyclohexene indicating the presence of substantial Brönsted acidity in the catalyst.

The DRIFT spectra of pyridine adsorbed SZ catalyst exhibited the characteristic peaks for pyridinium ion (Brönsted acid sites, B) at 1545 cm^{-1} and covalently bonded pyridine (Lewis acid sites, L) at 1442 cm^{-1} (Fig. 2) along with peak at 1489 cm^{-1} representing the combined B and L acid sites. The peaks at 1612 and 1637 cm^{-1} also showed the presence of L and B acid sites, respectively [38]. Both B and L acid sites were observed to be strong enough as they were present even after heating at 450 °C; though the intensity of the peaks was decreased after successive heating (Fig. 2). The quantification of B/L ratio, calculated from the characteristic peak area at 150 °C (B/L = 1.42) as well as by molar extinction coefficient method (B/L = 1.38; B = 0.044 mmol/g; L = 0.032 mmol/g) was in good agreement (Table 1). The results indicated the presence of significant amount of Brönsted acidity in the catalyst as also shown by cyclohexanol dehydration, a model reaction to access Brönsted acidity of solid acid catalysts.

3.2. Esterification of palmitic acid with methanol

The effect of various reaction parameters such as acid to methanol ratio, catalyst amount, temperature, time, stirring speed and alcohol chain length has been studied to optimize the reaction variables under the employed experimental conditions for achieving maximum yield of MP.

3.2.1. Effect of acid to methanol ratio

The reaction was studied with an acid to methanol molar ratio in the range of 1:5 to 1:30 over 1 wt% SZ catalyst (with respect to PA) at 60 °C for 7 h. The results showed 38% yield of MP with acid to methanol molar ratio of 1:5, which enhanced to 65% with successive increase in acid to methanol ratio to 1:20 (Fig. 3a). However, further increasing the acid to methanol ratio to 1:30, little decreased yield of MP (60%) was observed. It is assignable for the dilution effect as an optimum excess of methanol shifts the equilibrium of esterification reaction to the product side, however, further

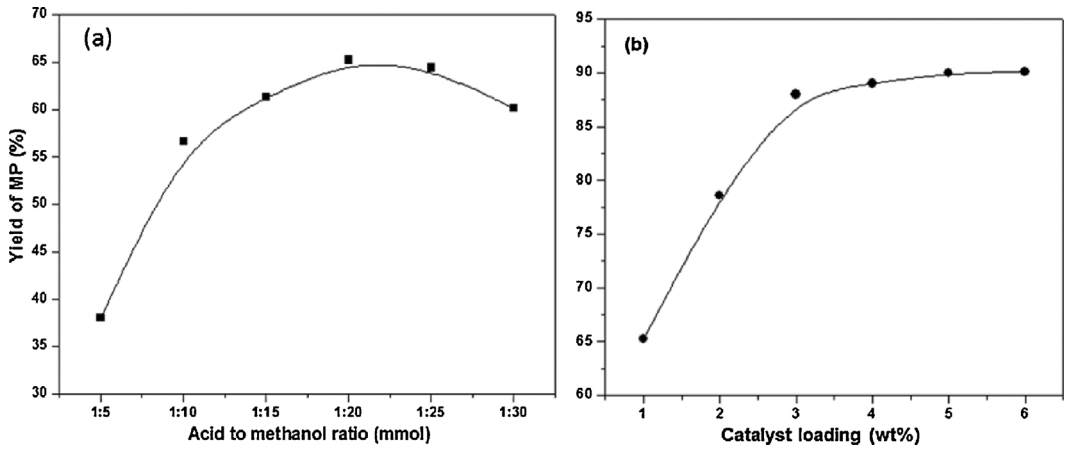

Fig. 3. Yield of methyl palmitate (MP) at varied (a) acid to methanol ratio (b) catalyst amount. Reaction conditions: temperature = 60 °C; time = 7 h; (a) catalyst = 1 wt%; (b) acid to methanol ratio = 20 (PA = 3 mmol and MeOH = 60 mmol).

excess deluges the active sites of the catalyst that may hinder the protonation of PA at the active sites and thus resulting into lower yield of the product. Hence, acid to methanol molar ratio of 1:20 was chosen for further study.

An excess of alcohol may lead to dehydration or etherification in the presence of strong acid catalyst such as sulfated zirconia. No such dehydrated or ether product was detected by GC–MS analysis under the reaction conditions studied.

The yield of MP calculated by ^{1}H NMR was found similar to the conversion of PA on the basis of acid value using acid base titration.

3.2.2. Effect of catalyst amount

A linear increase in the yield of MP from 65 to 88% was found by increasing the catalyst amount from 0.5 to 3 wt%. By further increasing the catalyst amount to 4–6 wt%, the yield was marginally increased to 90% (Fig. 3b). Therefore, 3 wt% was chosen as optimum catalyst amount, however, studies with 6 wt% catalyst have also been carried out.

3.2.3. Effect of reaction temperature

The SZ catalyst showed a gradual increase in the yield of methyl palmitate from 64 to 88% by increasing the temperature from 50 to 60 °C (Fig. 4a). This is probably due to better solubility and miscibility of PA with methanol at higher temperature (insoluble at room temperature and partially soluble at 50 °C), which facilitate the protonation of the carbonyl group of PA as well as lowers the mass transfer limit resulting in increased yield of product. As boiling point of methanol is 65 °C, we have studied all reactions at 60 °C to avoid any vapor loss.

3.2.4. Effect of stirring speed

To study the effect of mass transfer, the catalytic experiments were conducted at different stirring speeds (500–900 rpm). The results showed the yield of MP in the range of 89–90% at different stirring speed of 600–900 rpm, however at slower stirring speed of 500 rpm, the yield was slightly lower (86%) (Fig. 4b). These results indicated the absence of mass transfer resistance at >600 rpm and the reactions were in kinetic regime. To ensure the pure kinetic regime all experiments were performed at a constant stirring speed of 700 rpm.

3.2.5. Effect of alcohol chain length

The esterification of PA was also studied with other short chain alcohols besides methanol namely ethanol, *n*-propanol and *n*-butanol at the reflux conditions, near to the boiling point temperature of respective alcohol (75–115 °C). The result showed a successive decrease in the yield of corresponding ester from methyl palmitate to butyl palmitate (88–33%) under the optimized reaction conditions of acid to alcohol molar ratio to 1:20 with 3 wt% of SZ catalyst (Fig. 5). This is due to the inductive effect of increased carbon chain of alcohol. The electron donating ability of alkyl group toward the hydroxyl group increases with increasing the alkyl chain of

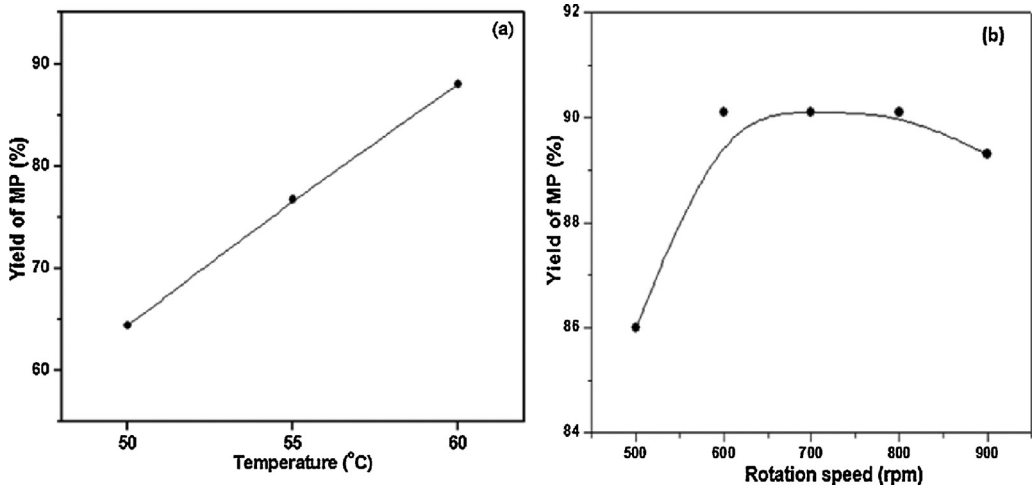

Fig. 4. Yield of methyl palmitate (MP) at varied (a) temperature (b) stirring speed. Reaction conditions: PA = 3 mmol and MeOH = 60 mmol; catalyst = 3 wt%; time = 7 h; (b) temperature = 60 °C.

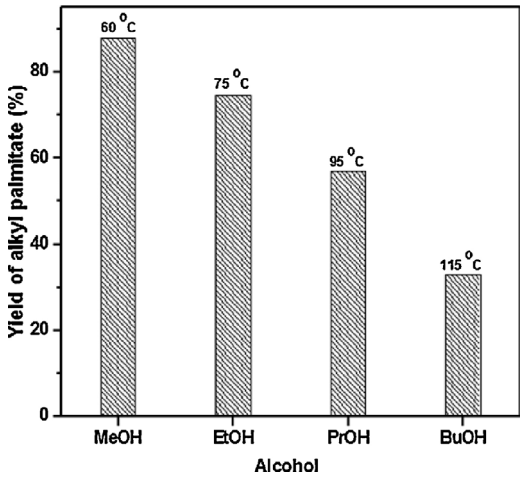

Fig. 5. Yield of methyl palmitate (MP) with various alcohols. Reaction conditions: PA = 3 mmol and ROH = 60 mmol; catalyst = 3 wt%; time = 7 h.

alcohol thus lowers the hydroxylation and limiting the electrophilic attack by the acid.

3.3. Kinetic studies

The kinetic profile of esterification reaction obtained with time in terms of the consumption of PA and formation of MP is given in Fig. 6a. A linear decrease in the concentration of PA was observed up to 60 min and on further increasing the time decrease in concentration of PA became slow and started to approach saturation. An identical trend in the formation of MP was obtained. Both the initial rates for the consumption of PA and formation of MP were determined by using following equations,

$$\nu = -\frac{d\,[\mathrm{PA}]}{\mathrm{dt}} \quad (1)$$

$$\nu_1 = \frac{d[\mathrm{MP}]}{\mathrm{dt}} \quad (2)$$

The rates ν and ν_1 were calculated from the early linear portion of the graph (Fig. 6a) from the decreasing concentration of PA and increasing concentration of MP, respectively. In typical experimental conditions as mentioned in Fig. 6a, both the rates ν (1.15 mmol h^{-1}) and ν_1 (1.13 mmol h^{-1}) were found to be almost identical indicating that there is a fine balance between the concentration of the consumption of PA and selective formation of MP. The kinetic investigations were performed by varying the amount of catalyst from 0.5 to 5 wt% by keeping other reaction conditions and concentration of PA constant for a representative alcohol methanol. The effect of variation in catalyst amount with respect to formation of MP is given in Fig. 6b and the corresponding rates (ν_1) are given in Fig. 7a. The rate of formation of MP was increased by increasing the catalyst amount (0.5 to 3 wt%) showing first order dependent toward lower amount of the catalyst. By further increasing the amount of the catalyst (5 wt%), the rate tends to attain the saturation. In order to observe the kinetic dependence of the substrates, the experiments carried out under typical conditions with 1:20 molar ratio of PA and methanol over 3 wt% of catalyst gave a very good fitness of pseudo-first order kinetics in the plot of ln [PA] versus time (Fig. 7b). The pseudo-first order rate constant k (h^{-1}) determined at different catalyst amount were: $k \times 10^2$ (wt%) = 1.24 (0.5), 2.34 (1.0), 7.20 (3.0) and 7.60 (5.0). These rate constants were also increased in the line of the increasing of the rates (ν_1) on increasing the catalyst amount indicating first order dependence on the catalyst amount.

The reaction rate per gram of catalyst with 3 wt% SZ catalyst was observed to be 48.67 mmol h^{-1} g^{-1}. Turnover frequency (TOF, mmol of palmitic acid converted per mole of acid site concentration per hour) was found to be 6.96 h^{-1}. It is noteworthy that TOF of the present study over SZ catalyst was found similar to conc. H_2SO_4 (6.78 h^{-1}) for the similar reaction [22], which clearly demonstrates the efficiency of SZ heterogeneous catalyst as a suitable replacement for homogeneous sulfuric acid.

The results clearly demonstrate that higher Brönsted acidic nature of SZ catalyst combined with mesoporosity and good structural, textural features displays higher catalytic activity for the studied reaction.

3.4. Re-usability of SZ catalyst

The re-usability of SZ catalyst was examined by carrying out successive reaction cycles. After each cycle, the catalyst was recovered from the reaction mixture by centrifugation and washed by methanol/methanol and hexane solution (~1:1) under ~2-3 min sonication to remove the PA/MP adhered on catalyst surface. The washed catalyst was re-calcined at 600 °C before its re-use for a new reaction cycle with fresh reactants. The results (Fig. 8) showed a successive decrease (from 88 to 36%) in the yield of MP after five reaction cycles when methanol was used as a solvent to wash the catalyst, however, the yield was significantly improved by using methanol and hexane solution for washing the catalyst. The catalyst revealed a slight decrease in the yield of MP during successive three reaction cycles (75%) after which the yield was steady till five reaction cycles (71%). The deactivation of SZ catalyst has been reported due to (i) water molecules formed as a by-product during

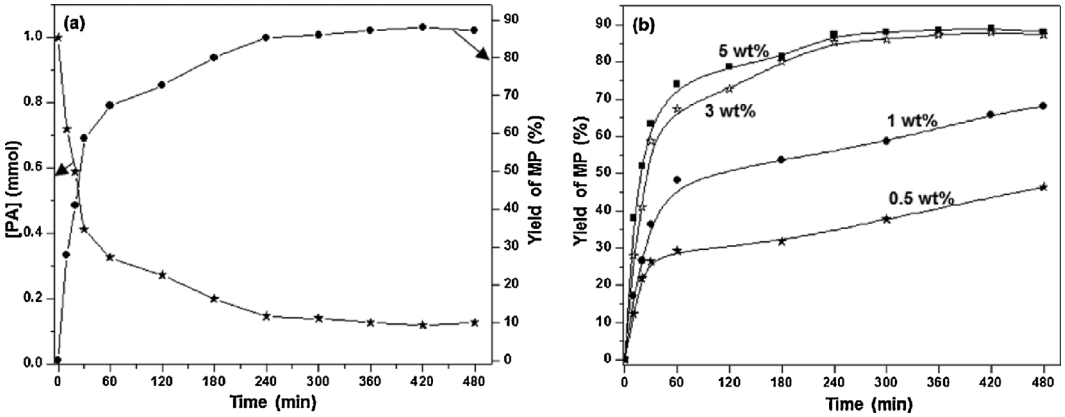

Fig. 6. Reaction profile for esterification of palmitic acid (PA) with time (a) over 3 wt% and (b) yield of methyl palmitate (MP) over varied catalyst amount. Reaction conditions: PA = 3 mmol and MeOH = 60 mmol; temperature = 60 °C.

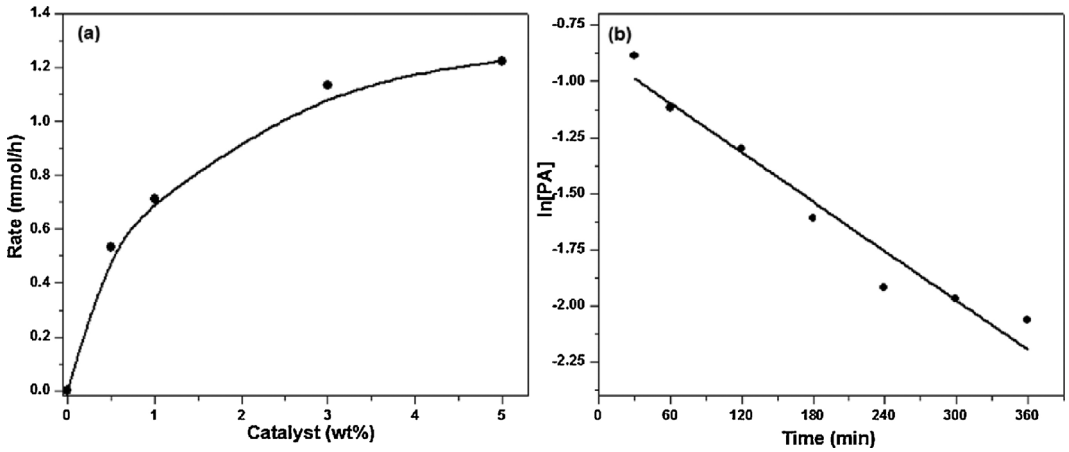

Fig. 7. (a) Rate of esterification reaction of palmitic acid (PA) with methanol versus catalyst amount (b) reaction rate constant over 3 wt% catalyst.

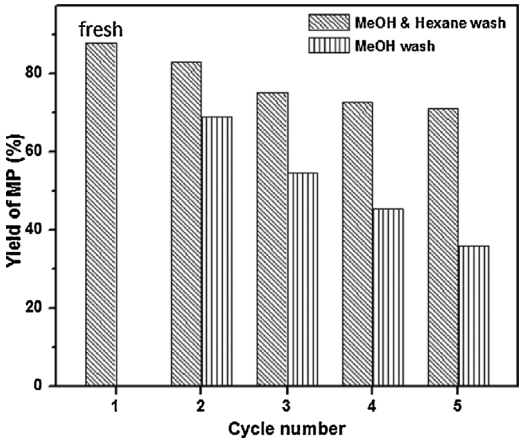

Fig. 8. Re-cyclability of SZ catalyst for esterification of palmitic acid (PA) with methanol. Reaction conditions: PA = 3 mmol and MeOH = 60 mmol; temperature = 60 °C; time = 5 h.

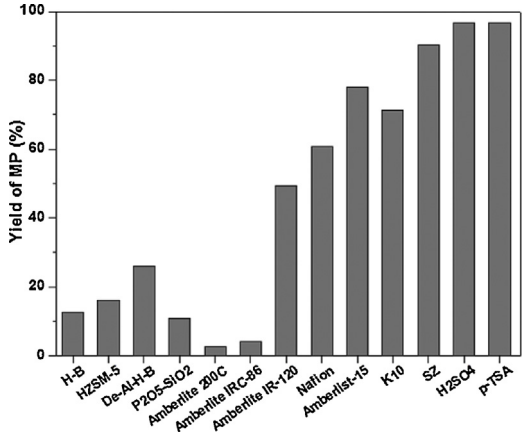

Fig. 9. Esterification of palmitic acid (PA) with methanol over various heterogeneous and homogeneous acid catalysts. Reaction conditions: PA = 3 mmol and MeOH = 60 mmol; catalyst amount = 6 wt%; temperature = 60 °C; time = 7 h.

the esterification reaction because of having high proton affinity and so hinder the interaction of reactants with acid sites [39], (ii) blockage of acid sites by adsorbed organic species [39] and (iii) leaching of sulfate species [39,40].

We have studied the leaching of sulfate during the reaction by removing the SZ catalyst after 30 min of the reaction and continued the reaction without catalyst till 5 h. The yield of MP was 59% after 30 min and increased only 67% after 5 h in absence of catalyst, which was significantly lower than 88–90% yield of MP in presence of catalyst (Fig. S5). The blank reaction (without catalyst) also showed ~3% yield of MP after 5 h. Therefore, this minor increase (~8%) in the yield of MP after removing the catalyst may occur due to autocatalysis along with sulfate leached during the reaction. The elemental analysis of the reaction mixtures of subsequent five reaction cycles during the re-usability studies showed the absence of sulfur content. However, sulfur content of the catalyst (after five reaction cycles) was found to decrease (0.26 mmol/g). The carbon of fresh and used catalyst was found similar (0.1 wt%) indicating no blockage of acid sites by carbon deposition. Therefore, the slight decrease in the catalyst activity may be attributed to loss of sulfate species.

4. Comparison of catalytic activity of SZ with other heterogeneous catalysts

We have studied the esterification of PA with methanol over various heterogeneous catalysts such as ion-exchange resins, zeolites, K10 acid clay, homogeneous Brönsted acids namely H_2SO_4 and *p*-TSA and compared the activity with SZ catalyst under optimized reaction conditions. The results (Fig. 9) showed that among ion-exchange resins, Amberlite IRC-86 and Amberlite 200 C exhibited very low yield (3–4%) of MP due to their weak acidic nature, which was enhanced to 49% by using a strong acid resin, Amberlite IR-120. The sulfonic ion-exchange resins namely Nafion SAC-13 and Amberlyst-15 catalysts showed 61–78% yield. Amberlyst-15 is one of the macroporous polystyrene/divinylbenzene sulfonic ion-exchange resins, while Nafion SAC-13 is a composite material, combining Nafion and a porous silica.

Zeolites H–β and HZSM-5 (Si/Al = 24) catalysts resulted into lower yield of 13–16%. Dealumination of zeolite H–β (De–Al–H–β) also could result only 26% yield (Fig. 9). Zeolites are microporous (<2 nm) crystalline solids having internal diffusion limitations of the bulky fatty acid/ester molecules and thus are not suitable for the synthesis of fatty acid alkyl ester. However, K10 acid clay, having layered structure, showed good activity with 71% MP yield. SiO_2 supported P_2O_5 exhibited only 11% yield of MP (Fig. 9).

Homogeneous Brönsted acid namely H_2SO_4 and *p*-TSA showed higher yield (95–97%) (Fig. 9); however, use of eco-friendly heterogeneous catalysts is advantageous due to easy separation and re-use of the catalyst. In general, among all the heterogeneous catalysts studied, SZ catalysts exhibited highest catalytic activity (88–90%) under the present reaction conditions, which was comparable to conventional homogeneous Brönsted acids.

5. Conclusions

Sulfated zirconia solid acid catalyst having higher Brönsted acidity, mesoporosity and good structural, textural features exhibited an excellent activity for the esterification of palmitic acid with methanol showing 88–90% yield of methyl palmitate at 60 °C. The yield of corresponding ester from methyl palmitate to butyl palmitate was decreased due to increasing carbon chain of alcohols. The reaction follows pseudo-first order kinetics under the optimized reaction conditions with a reaction rate of 48.67 mmol h^{-1} g^{-1} and TOF of 6.96 h^{-1} over 3 wt% catalyst concentration. Among various heterogeneous catalysts studied such as zeolites, ion exchange resins and acid clay, SZ catalysts showed higher activity for the studied reaction. In addition, its activity was found to be comparable to conventional homogeneous Brönsted acids such as H_2SO_4 and *p*-TSA under the optimized reaction conditions, which unambiguously demonstrates its efficiency to replace the conventional homogeneous Brönsted acid catalysts.

Acknowledgements

CSIR-CSMCRI communication No. 143/2014. Authors are thankful to CSIR Network Programme on Clean Coal Technology (TapCoal-0102) and to 'Analytical Discipline and Centralized Instrumental Facilities' for providing instrumentation facilities and Dr. M.K. Mishra, D. D. University, Nadiad, Gujarat for ion chromatography analysis. K. Saravanan is thankful to AcSIR for enrolment in PhD. Authors are thankful to reviewers for their comments and valuable suggestions.

Appendix A. Supplementary data

Supplementary data associated with this article can be found, in the online version, at http://dx.doi.org/10.1016/j.apcatb.2015.02.014.

References

[1] I.K. Mbaraka, D.R. Radu, V.S.-Y. Lin, B.H. Shanks, J. Catal. 219 (2003) 329–336.
[2] I.B. Banković-Ilić, O.S. Stamenković, V.B. Veljković, Renew. Sust. Energ. Rev. 16 (2012) 3621–3647.
[3] E. Lotero, Y.J. Liu, D.E. Lopez, K. Suwannakaran, D.A. Bruce, J.G. Goodwin Jr., Ind. Eng. Chem. Res 44 (2005) 5353–5363.
[4] E. Crabbe, C. Nolasco-Hipolito, G. Kobayashi, K. Sonomoto, A. Ishizaki, Process Biochem. 37 (2001) 65–71.
[5] http://en.wikipedia.org/wiki/Palmitic_acid
[6] G.D. Yadav, M.S.M. Mujeebur Rahuman, Clean Tech. Environ. Policy 5 (2003) 128–135.
[7] J.H. Clark, Acc. Chem. Res. 35 (2002) 791–797.
[8] J.A. Melero, J. Iglesias, G. Morales, Green Chem. 11 (2009) 1285–1308.
[9] (a) A.A. Kiss, A.C. Dimian, G. Rothenberg, Adv. Synth. Catal. 348 (2006) 75–81; (b) A.A. Kiss, F. Omata, A.C. Dimian, G. Rothenberg, Top Catal. 40 (2006) 141–150.
[10] J.A.A. Takagaki, M. Toda, M. Okamura, J.N. Kondo, K. Domen, S. Hayashi, M. Hara, Catal. Today 116 (2006) 157–161.
[11] Y.F. Feng, X.Y. Yang, D. Yang, Y.C. Du, Y.L. Zhang, F.S. Xiao, J. Phys. Chem. B 110 (2006) 14142–14147.
[12] J.K. Satyarthi, D. Srinivas, P. Ratnasamy, Energy Fuels 24 (2010) 2154–2161.
[13] L. He, S. Qin, T. Chang, Y. Sun, X. Gao, Catal. Sci. Technol. 3 (2013) 1102–1107.
[14] S. Ramu, N. Lingaiaha, B.L.A.P. Devi, R.B.N. Prasad, I. Suryanarayanaa, P.S.S. Prasad, Appl. Catal. A 276 (2004) 163–168.
[15] C. Poonjarernsilp, N. Sano, H. Tamon, Appl. Catal. B 147 (2014) 726–732.
[16] V. Brahmkhatri, A. Patel, Ind. Eng. Chem. Res. 50 (2011) 6620–6628.
[17] A.C. Carmo, L.K.C. de Souza, C.E.F. da Costa, E. Longo, J.R. Zamian, G.N. da Rocha Filho, Fuel 88 (2009) 461–468.
[18] K.N. Rao, A. Sridhar, A.F. Lee, S.J. Tavener, N.A. Young, K. Wilson, Green Chem. 8 (2006) 790–797.
[19] B.L. Devi, K.N. Gangadhar, P.S. Prasad, B. Jagannadh, R.B. Prasad, ChemSusChem 2 (2009) 617–620.
[20] A. Baig, F.T.T. Ng, Energy Fuels 24 (2010) 4712–4720.
[21] (a) C.S. Caetano, M. Caiado, J. Farinha, I.M. Fonseca, A.M. Ramos, J. Vital, J.E. Castanheiro, Chem. Eng. J. 230 (2013) 567–572; (b) C.S. Caetano, L. Guerreiro, I.M. Fonseca, A.M. Ramos, J. Vital, J.E. Castanheiro, Appl. Catal. A 359 (2009) 41–46.
[22] A.I. Tropecêlo, M.H. Casimiro, I.M. Fonseca, A.M. Ramos, J. Vital, J.E. Castanheiro, Appl. Catal. A 390 (2010) 183–189.
[23] A. Dutta, A.K. Patra, H. Uyama, A. Bhaumik, ACS Appl. Mater. Interfaces 5 (2013) 9913–9917.
[24] C.S. Caetano, I.M. Fonseca, A.M. Ramos, J. Vital, J.E. Castanheiro, Catal. Commun. 9 (2008) 1996–1999.
[25] (a) K. Srilatha, N. Lingaiah, B.L.A.P. Devi, R.B.N. Prasad, S. Venkateswar, P.S.S. Prasad, Appl. Catal. A 365 (2009) 28–33; (b) B.Y. Giri, K.N. Rao, B.L.A.P. Devi, N. Lingaiah, I. Suryanarayana, R.B.N. Prasad, P.S.S. Prasad, Catal. Commun. 6 (2005) 788–792.
[26] J. de, A. Gonçalves, A.L.D. Ramos, L.L.L. Rocha, A.K. Domingos, R.S. Monteiro, J.S. Peres, N.C. Furtado, C.A. Taft, D.A.G. Aranda, J. Phys. Org. Chem. 24 (2010) 54–64.
[27] L. Roldán, I. Santos, S. Armenise, J.M. Fraile, E. Garcıá-Bordejé, Carbon 50 (2012) 1363–1372.
[28] (a) K. Saravanan, B. Tyagi, H.C. Bajaj, Catal. Sci. Technol. 2 (2012) 2512–2520; (b) K. Saravanan, B. Tyagi, H.C. Bajaj, Ind. J. Chem. A 53A (2014) 799–805.
[29] U. Ciesla, M. Fröba, G. Stucky, F. Schüth, Chem. Mater. 11 (1999) 227–234.
[30] B.D. Cullity, S.R. Stock, Elements of X-ray Diffraction, 3rd ed., Prentice Hall, Upper Saddle River, NJ, 2001, pp. p388.
[31] S.J. Gregg, K.S.W. Sing, Adsorption, Surface Area and Porosity, 2nd ed., Academic Press, New York, 1982.
[32] B. Tyagi, M.K. Mishra, R.V. Jasra, J. Mol. Cat. A: Chem. 286 (2008) 41–46.
[33] B. Tyagi, C.D. Chudasama, R.V. Jasra, Appl. Clay Sci. 31 (2006) 16–28.
[34] C.A. Emeis, J. Catal. 141 (1993) 347–354.
[35] T. Barzetti, E. Selli, D. Moscotti, L. Forni, J. Chem. Soc. Faraday Trans. 92 (1996) 1401–1407.
[36] J.K. Satyarthi, S. Radhakrishnan, D. Srinivas, Energy Fuels 25 (2011) 4106–4112.
[37] T. Yamaguchi, T. Jin, K. Tanabe, J. Phys. Chem. 90 (1986) 3148–3152.
[38] H. Armendariz, M.A. Cortes, I. Hernandez, J. Navarrete, A. Vazquez, J. Mater. Chem. 13 (2003) 143–149.
[39] J. Ni, F.C. Meunier, Appl. Catal. A: Gen. 333 (2007) 122–130.
[40] I. Dosuna-Rodríguez, C. Adriany, E.M. Gaigneaux, Catal. Today 167 (2011) 56–63.